Figure S1

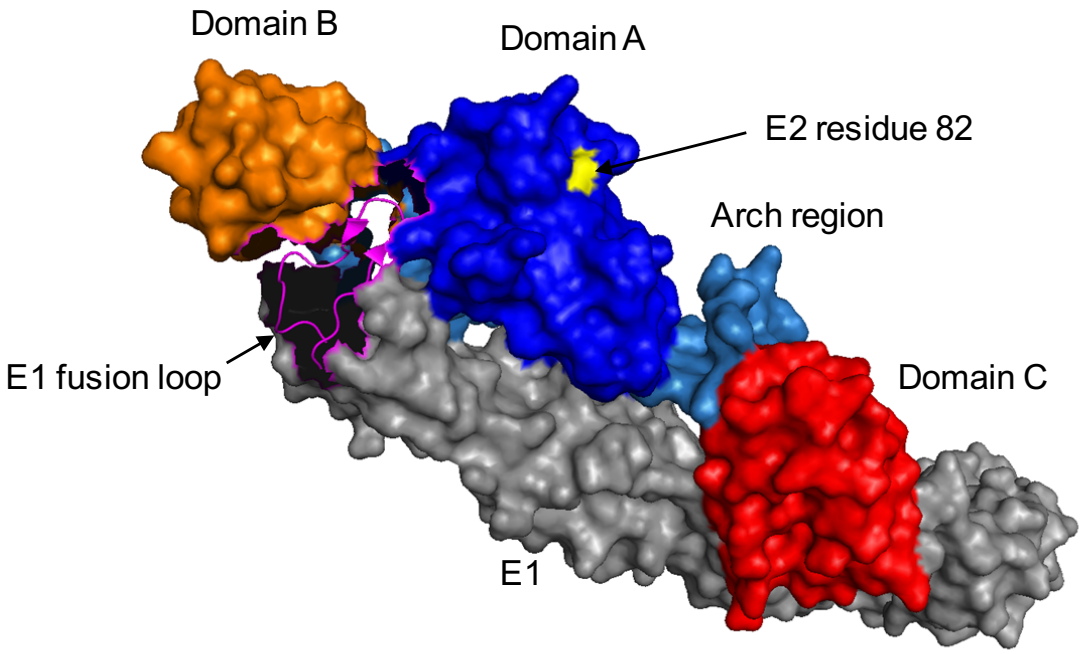

Supplemental Figure 1, related to Figure 7. Organization of the CHIKV E2-E1 heterodimer. Surface view of the CHIKV E2 and E1 heterodimer (PDB: 3N42; Voss et al. 2010). E1 is colored light grey, the E1 fusion loop is colored pink, E2 domain A is colored dark blue, E2 domain B is colored orange, E2 domain C is colored red, the E2 arch regions are colored light blue, and residue at E2 position 82 is colored yellow.

Figure S2

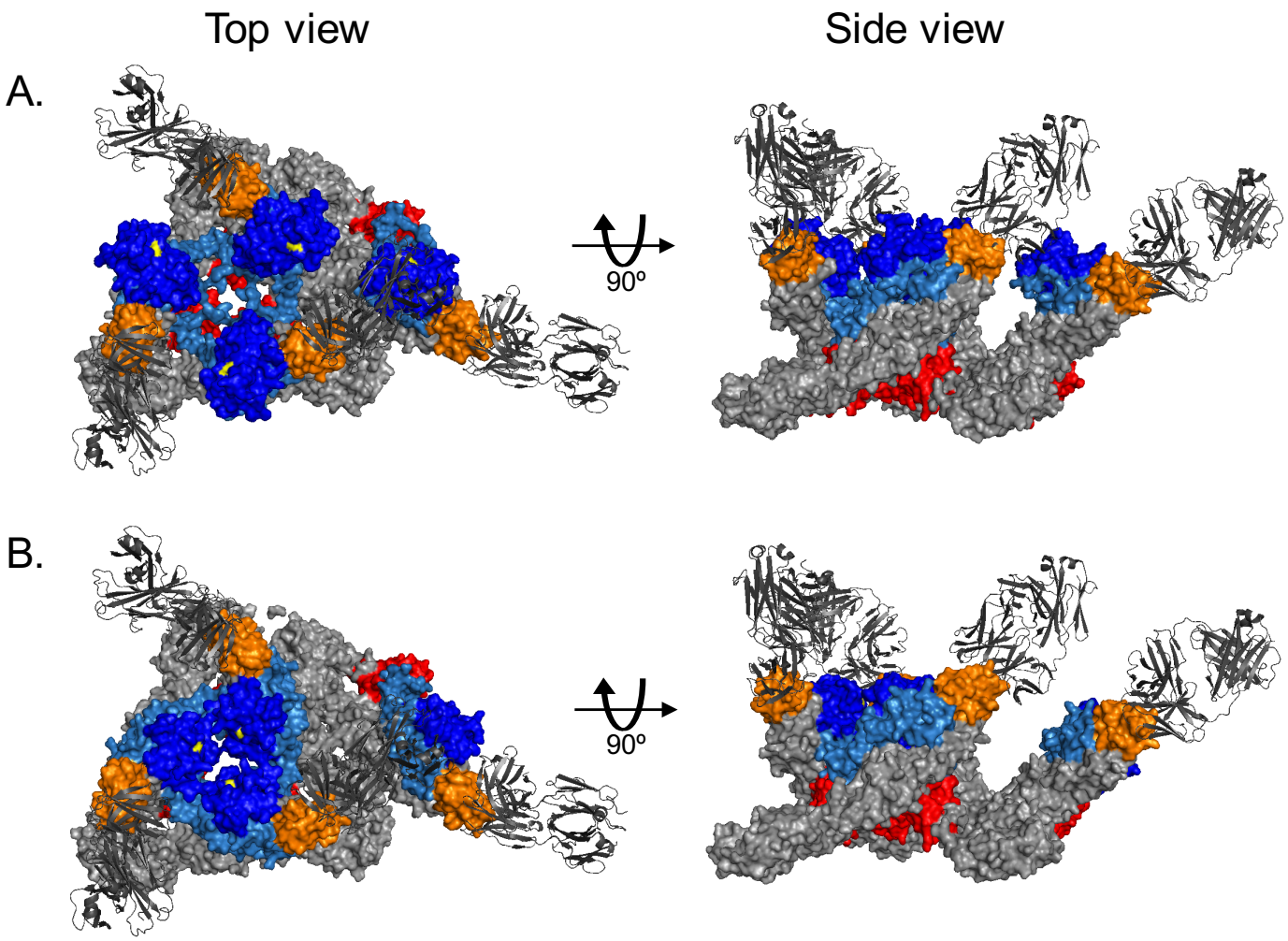

Supplement Figure 2, related to Figures 5, 6, and 7. Possible model of how E2 residue 82 influences virus neutralization by antibodies that target the E2 B domain.
(A) Cryo-EM reconstruction of CHIKV 181/25 in complex with CHK-265 Fab fragments (PDB: 5ANY; Fox et al. 2015). The CHK-265 Fab molecules are colored dark grey, E1 is colored light grey, E2 domain A is colored dark blue, E2 domain B is colored orange, E2 domain C is colored red, the E2 arch regions are colored light blue, and the arginine (R) residue at E2 position 82 is colored yellow.
(B) CHK-265 Fab fragments in complex with a CHIKV strain encoding a glycine (G) residue at E2 position 82 (yellow) was modeled based on data reported under PDB: 2XFC (Voss et al. 2010). In this model, the interactions between CHK-265 and the A domain of E2 in a neighboring trimeric spike that occur when CHK-265 is complexed with viruses encoding an R at E2 position 82 (as shown in A) may occur less efficiently. Note the potential change in position of E2 residue 82 within the core of the trimeric spike, the change in position of domain A, and the increased space between E2 molecules of neighboring trimeric spikes in comparison with the reconstruction shown in (A).

Supplemental Experimental Procedures

Cells. Baby hamster kidney cells (BHK-21; ATCC CCL-10) were maintained in ✔-Minimal Essential Medium (MEM) supplemented with 10% fetal bovine serum (FBS), 10% tryptose phosphate, 2 mM L-glutamine, 100 U/ml penicillin, and 100 µg/ml streptomycin. Vero cells (ATCC CCL-81) were maintained in Dulbecco's Modified Eagle Medium/F12 supplemented with 10% FBS, non-essential amino acids, 100 U/ml penicillin, and 100 µg/ml streptomycin.

Viruses. Plasmids encoding infectious cDNA clones of CHIKV strains SL15649, AF15561, and 181/25 have been described (Ashbrook et al., 2014; Morrison et al., 2011). Generation of virus stocks from cDNA clones was performed as described (Morrison et al., 2011). Plasmids were linearized and used as a template for in vitro transcription with SP6 DNA-dependent RNA polymerase (Ambion). RNA was electroporated into BHK-21 cells and at 24 h post-electroporation, supernatant was collected and clarified by centrifugation at 1,721 x g. Clarified supernatants were aliquoted and stored at -80°C. Viral titers were determined by plaque assays on BHK-21 and Vero cells as described (Hawman et al., 2013).

Site-directed mutagenesis. Site-directed mutagenesis to introduce mutations into the 181/25 or SL15649 cDNA was performed using the Quick Change II XL site-directed mutagenesis kit (Agilent). Plasmids were sequenced to verify that only the desired mutations were present.

Mouse experiments. WT, Rag1$^{-/-}$, and µMT C57BL/6J mice were obtained from the Jackson Laboratory. Tg(IghelMD4)4Ccg/J (MD4^{tr}) C57BL/6J mice which encode a B cell receptor specific for hen egg lysozyme were provided by John C. Cambier (University of Colorado School of Medicine). All mice were bred in specific-pathogen-free facilities at the University of Colorado Anschutz Medical Campus. Three-to-four week-old mice were used for all studies. Mice were inoculated in the left rear footpad with virus in diluent (phosphate-buffered saline [PBS] supplemented with 1% FBS) in a volume of 10 µl. On the termination day of each experiment, mice were sedated with isoflurane and euthanized by thoracotomy, blood was collected, and mice were perfused extensively by intracardiac injection of PBS. Serum was obtained by collecting blood in serum separator tubes (BD). PBS-perfused tissues were removed by dissection, placed into TRIzol reagent (Life Technologies) for RNA isolation or PBS-1% FBS for tissue titers and homogenized using a MagNA Lyser (Roche). Animal husbandry and experiments were

performed in accordance with all University of Colorado School of Medicine Institutional Animal Care and Use Committee guidelines. All mouse studies were performed in an animal biosafety level 3 laboratory.

Quantification of viral RNA. Viral RNA was quantified by RT-qPCR as described (Hawman et al., 2013). Mouse tissues were dissected into TRIzol and total RNA isolated using the Pure Link RNA kit (Life Technologies). cDNA was generated using the Super Script III first strand-synthesis system (Life Technologies) and 1 µg of RNA primed with 250 ng of random primers (Life Technologies). The number of genomes was then quantified via quantitative PCR using a CHIKV sequence-specific forward primer (CHIKV2411, 5'-AGAGACCAGTCGACGTGTTGTAC-3') and a CHIKV sequence-specific reverse primer (CHIKV2676, 5'-GTGCGCAT TTTGCCTTCGTA-3') in conjunction with a CHIKV sequence-specific TaqMan probe (CHIKV2579, 5'-FAM-ATCTGCACCCA AGTGTACCA-MGB-3') on a LightCycler480 (Roche). Absolute quantification was performed by comparison to an internal standard curve. The standard curve was generated by spiking serial 10-fold dilutions of in vitro transcribed viral RNA into excess BHK-21 RNA; cDNA was generated and quantified in an identical manner. Values are expressed as the copy number per 1 µg of input RNA into the cDNA reaction. No template controls were included in parallel to ensure assay specificity. The limit of detection was 100 copies of CHIKV RNA per ug of total RNA. To quantify viral RNA copies in stocks of infectious virus, a modified reverse transcription protocol was used in which 5 µl of a 1:100 dilution of virus stock in water was incubated with 250 ng random primers at 94°C for 5 min followed by 70°C for 5 min prior to the reverse-transcription reaction (Jupille et al., 2013; Snyder et al., 2012). qPCR was then performed as above.

Sequencing of viral RNA in mouse tissues. Random primed cDNA was amplified by PCR amplified using Q5 high-fidelity polymerase (NEB). Primers used were CHIKV8400, 5'- CTCCCAGCCCCCTTGCAC and CHIKV8889, 5'- AGTGAATCCCACCGTCAGAGTT. PCR reactions were purified using the QIAquick PCR clean-up kit (Qiagen) and submitted for Sanger sequencing. Reads were aligned to the reference 181/25 genome (Genbank: L37661.3) using Geneious software (Biomatters). No template controls were included in parallel for all reactions.

Quantification of infectious virus in tissues. PBS-perfused tissues were dissected into PBS/1% FBS and homogenized as described above. Tissue homogenates were clarified by centrifugation (17,000 x g) and the supernatant was used in a standard BHK-21 cell plaque assay (Morrison et al., 2011).

Enzyme-linked immunosorbant assay. To quantify CHIKV-binding antibodies in mouse sera (collected from mock-infected, as a control, and CHIKV-infected mice), a virion enzyme-linked immunosorbant assay (ELISA) was performed. Virus used in the ELISA was generated by passaging AF15561 or 181/25 once in BHK-21 cells. Cell culture supernatants from these infections were concentrated via ultra-centrifugation at 24,000 RPM in SW-32ti rotor through a 20% sucrose cushion. Virus pellets were resuspended in PBS and the genomes per ml were quantified by RT-qPCR as described above. 1.25 x 10^8 genomes (particles) diluted in PBS were adsorbed overnight at 4°C to wells in a 96-well Immulon 4HBX plate (Thermo Scientific). Following adsorption, wells were blocked with Super Block in PBS (Thermo Scientific) and two-fold serial dilutions of serum were applied to the plate. After incubation at room temperature for 1 h, plates were washed with PBS + 0.05% Tween-20 and incubated with biotin-conjugated goat anti-mouse IgM or IgG antibodies (1:4000; Southern Biotech) followed by streptavidin conjugated to horseradish peroxidase (1:4000; Southern Biotech). Plates were developed with 3,3′,5,5′-tetramethylbenzidine liquid substrate (Sigma) and the reaction stopped with 0.3 N sulfuric acid. Absorbance was read at 450 nM using a Biotek spectrophotometer. Endpoint titers were defined as the reciprocal of the last dilution to have an absorbance two times greater than background. As internal negative controls, IgG and IgM were measured against uninfected BHK-21 cell antigen absorbed to wells for each serum sample. As an internal positive control, a CHIKV monoclonal IgG antibody (CHK-152) (Pal et al., 2013) was applied (1:250,000) and developed with IgG detection antibodies. Blank wells receiving no serum were used to measure background signal.

Plaque reduction neutralization test. For analysis of neutralizing activity, a plaque reduction neutralization test (PRNT) was performed. Serum was heat-inactivated at 56°C for 30 min and serially diluted in PBS + Ca^{2+} + Mg^{2+} + 2% heat-inactivated FBS beginning with the 1:8 dilution. Diluted serum samples were incubated with an equal volume of 50 PFU of challenge virus at 37°C for 1 h. Following incubation, samples were adsorbed on Vero cells at 37°C for 1 hr, followed by an overlay with 0.5% immunodiffusion agarose (MP Biomedicals) in medium for 38 to 40 h. Plaques were visualized by neutral red staining (Sigma). Plaque numbers were enumerated to determine the number of PFU per ml. To calculate percent infectivity, the challenge virus was incubated in PBS + Ca^{2+} + Mg^{2+} + 2% heat-inactivated FBS alone in parallel to serum samples and data reported as (# of plaques in serum-treated samples/# of plaques in input) x 100. The $PRNT_{50}$ value was defined as the reciprocal of the last dilution to exhibit < 50% infectivity.

Focus reduction neutralization test. Serial dilutions of MAb were incubated with 100 FFU of CHIKV at 37°C for 1 h, as previously described (Pal et al., 2013). MAb-virus complexes were added to cells in 96-well plates. After 90 min, cells were overlaid with 1% (w/v) methylcellulose in Modified Eagle Media (MEM) supplemented with 4% FBS. Plates were harvested 18 to 24 hours later, and fixed with 1% PFA in PBS. The plates were incubated sequentially with 500 ng/ml of ch-CHK-9 or CHK-11 (Pal et al., 2013) and horseradish peroxidase (HRP)-conjugated goat anti-human IgG in PBS supplemented with 0.1% saponin and 0.1% bovine serum albumin. CHIKV-infected foci were visualized using TrueBlue peroxidase substrate (KPL) and quantified on an ImmunoSpot 5.0.37 macroanalyzer (Cellular Technologies Ltd). Non-linear regression analysis was performed, and EC_{50} values were calculated after comparison to wells infected with CHIKV in the absence of antibody.

References

Ashbrook, A.W., Burrack, K.S., Silva, L.A., Montgomery, S.A., Heise, M.T., Morrison, T.E., and Dermody, T.S. (2014). Residue 82 of the Chikungunya virus E2 attachment protein modulates viral dissemination and arthritis in mice. Journal of virology 88, 12180-12192.

Hawman, D.W., Stoermer, K.A., Montgomery, S.A., Pal, P., Oko, L., Diamond, M.S., and Morrison, T.E. (2013). Chronic joint disease caused by persistent Chikungunya virus infection is controlled by the adaptive immune response. Journal of virology 87, 13878-13888.

Jupille, H.J., Medina-Rivera, M., Hawman, D.W., Oko, L., and Morrison, T.E. (2013). A tyrosine-to-histidine switch at position 18 of the Ross River virus E2 glycoprotein is a determinant of virus fitness in disparate hosts. Journal of virology 87, 5970-5984.

Morrison, T.E., Oko, L., Montgomery, S.A., Whitmore, A.C., Lotstein, A.R., Gunn, B.M., Elmore, S.A., and Heise, M.T. (2011). A mouse model of chikungunya virus-induced musculoskeletal inflammatory disease: evidence of arthritis, tenosynovitis, myositis, and persistence. The American journal of pathology 178, 32-40.

Pal, P., Dowd, K.A., Brien, J.D., Edeling, M.A., Gorlatov, S., Johnson, S., Lee, I., Akahata, W., Nabel, G.J., Richter, M.K., et al. (2013). Development of a highly protective combination monoclonal antibody therapy against Chikungunya virus. PLoS pathogens 9, e1003312.

Snyder, A.J., Sokoloski, K.J., and Mukhopadhyay, S. (2012). Mutating conserved cysteines in the alphavirus e2 glycoprotein causes virus-specific assembly defects. Journal of virology 86, 3100-3111.